Int J Mech Mater Des (2012) 8:89–100
DOI 10.1007/s10999-012-9179-5

A mixed semi analytical solution for functionally graded (FG) finite length cylinders of orthotropic materials subjected to thermal load

P. Desai · T. Kant

Received: 21 July 2011 / Accepted: 5 January 2012 / Published online: 20 January 2012

Abstract A simplified and accurate analytical cum numerical model is presented here to investigate the behavior of functionally graded (FG) cylinders of finite length subjected to thermal load. A diaphragm supported FG cylinder under symmetric thermal load which is considered as a two dimensional (2D) plane strain problem of thermoelasticity in (r, z) direction. The boundary conditions are satisfied exactly in axial direction (z) by taking an analytical expression in terms of Fourier series expansion. Fundamental (basic) dependent variables are chosen in the radial coordinate of the cylinder. First order simultaneous ordinary differential equations are obtained as mathematical model which are integrated through an effective numerical integration technique by first transforming the boundary value problem into a set of initial value problems. For FG cylinders, the material properties have power law dependence in the radial coordinate. Effect of non homogeneity parameters and orthotropy of the materials on the stresses and displacements of FG cylinder are studied. The numerical results obtained are also first validated with existing literature for their accuracy. Stresses and displacements in axial and radial directions in cylinders having various l/r_i and $r_\mathrm{o}/r_\mathrm{i}$ ratios parameter are presented for future reference.

P. Desai (✉) · T. Kant
Department of Civil Engineering, Indian Institute of Technology Bombay, Powai, Mumbai 400 076, India
e-mail: payaldesai79@gmail.com

Keywords Functionally graded materials · Numerical Integration · Boundary value problems · Thick cylinder

List of symbols

r, θ, z	Cylindrical coordinates
u, v, w	Displacement components
σ_r, σ_θ, σ_z	Normal stress components on planes normal to r, θ, and z axis
τ_{zr}	Shearing stress component in cylindrical coordinates
ε_r, ε_θ, ε_z	Unit elongations (normal strain) components in cylindrical coordinates
γ_{zr}	Shearing strain component in cylindrical coordinates
C_{ij}	Material constants for orthotropic materials
α_i	Coefficient of thermal expansion per degree centigrade for orthotropic materials
T	Temperature rise at any point in a cylinder
v	Poisson's ratio
r_i	Inner radius of the cylinder
r_o	Outer radius of the cylinder
l	Length of the cylinder
T_m	Initial reference temperature
$\bar{u}, \bar{w}$	Nondimensionalized displacement components
$\overline{\sigma_r}, \overline{\sigma_\theta}, \overline{\sigma_z}$	Nondimensionalized normal stress components
$\overline{\tau_{rz}}$	Nondimensionalized shearing stress component in cylindrical coordinates

$\overline{r}$	Nondimensionalized radius
R	Mean radius $(r_o/r_i)/2$

1 Introduction

The demand for improved structural efficiency in space structures and nuclear reactors has resulted in the development of a new class of materials, called functionally graded materials (FGMs). FGMs have become one of the major research topics in the mechanics of materials community during the past 15 years. The concept of FGMs was proposed in 1984 by materials' scientists in the Sendai (Japan) area as a means of preparing thermal barrier materials (Koizumi 1997). Continuous changes in the composition, microstructure, porosity, etc. of these materials result in gradients in properties such as mechanical strength and thermal conductivity. Thus, FGMs are heterogeneous materials, characterized by spatially variable microstructures, and thus spatially variable macroscopic properties are introduced to enhance material or structural performance. Particularly, material properties can be designed to vary continuously along structural geometry to prevent delamination and stress concentration in traditional multilayered structures. The basic concept is to mix ceramic and metal such that the material properties continuously vary from one constituent material to the other. The spatially variable material properties make FGMs challenging to analyze. Before these material devices are used in engineering design, it is very important that these are analyzed very accurately. For such a reason, present study focuses the analysis of functionally graded (FG) cylinders using the exact approach. The uniqueness of this approach is: it first requires algebraic manipulation of basic elasticity equations like equilibrium, strain displacement and constitute equations. After this manipulation, this becomes the two point boundary value problem (BVP) which governs the behavior of finite length cylinder which is plane strain two dimensional problem in r, z plane and gives four first order simultaneous partial differential equations. This can be explained by the following equation (Kraus 1967; Goldberg et al. 1965).

$$y'(r) = A(r)y(r) + p(r) \tag{1}$$

In the domain, $r_1 \leq r \leq r_2$, where, $y(r)$ is an n-dimensional vector of dependent variables; dependent variables in the present case can be described as $\underline{y} = (u, w, \sigma_r, \tau_{rz})^t$. Choice of dependent variables is an important task. The variables which naturally appear on $r =$ constant are chosen as dependent variables; such variables are called intrinsic variables. Remaining variables are described as auxiliary dependent variables which are dependent on intrinsic dependent variables. $A(r)$ is a coefficient matrix of partial differential equations. $p(r)$ is an n-dimensional vector of non homogeneous (loading) terms. For boundary conditions, any $n/2$ elements of $y(r)$ are specified at the two termini edges; mixed type of boundary conditions can be specified in this type of formulation. Recently, Desai and Kant (2011) have obtained accurate stresses in laminated finite length cylinders subjected to thermo elastic load using similar numerical model. Research results obtained thus far have demonstrated that FGMs have great potential for improving material/structural performance in many engineering applications precisely because of their spatially graded heterogeneous microstructure. Some of the recent literature relevant in this study is described as follows. Horgan and Chan (1999) investigated the effects of material inhomogeneity in fundamental boundary-value problem of linear inhomogeneous isotropic pressurized hollow cylinder. The results are illustrated using a specific radially inhomogeneous material model for which explicit exact solutions are obtained. Chen et al. (2002) considered the axisymmetric thermoelastic problem of a uniformly heated, functionally graded isotropic hollow cylinder and proposed an analytical form of solution. Ye et al. (2001) studied the one-dimensional axisymmetric thermoelastic problem of a functionally graded transversely isotropic cylindrical shell and presented useful discussion and numerical results. Exact and explicit solution is derived. Tutuncu and Ozturk (2001) obtained closed-form solutions for stresses and displacements in functionally graded cylindrical and spherical vessels subjected to internal pressure alone using the infinitesimal theory of elasticity. Jabbari et al. (2002) developed a general analysis procedure for tackling one-dimensional steady-state thermal stress problem of a hollow thick cylinder made of FGMs. Recent literature survey follows will focus on FG cylinders of orthotropic materials subjected to thermal loads. Literature survey will focus on FG cylinders of orthotropic materials subjected to thermal loads.

Wu and Tsai (2011) have recently presented the three-dimensional (3D) coupled analysis of simply supported FG and piezoelectric sandwich cylinders under electro mechanical loads using modified pagano method. The modification in the original pagano's method were replacement of displacement-based formulation with mixed formulation and set of complex-valued solutions of system equation is transferred to a corresponding set of real-valued solutions. A transfer matrix method is used to analyse the effect of layers. Chen and Lin (2010) have analysed FG spheres with arbitrary Young's modulus and constant Poisson's ratio. Again the method of transmission matrix is used to account the effect of layers and continuity conditions are required in this paper Shariyat et al. (2011) developed analytical and numerical elastodynamic solutions for long thick walled functionally graded cylinders subjected to arbitrary dynamic and shock pressures. Liew et al. (2003) presented an analysis of the thermomechanical behavior of hollow circular cylinders of FGM. The solutions are obtained by a novel limiting process that employs the solutions of homogeneous hollow circular cylinders, with no recourse to the basic theory or the equations of non-homogeneous thermoelasticity. Yas and Aragh (2010) have investigated 3-D steady-state response of simply supported FG fiber reinforced cylindrical panel. Suitable temperature and displacement functions that identically satisfy the simply supported boundary conditions are used to reduce the thermoelastic equilibrium equations to a set of coupled ordinary differential equations (ODEs) with variable coefficients, which can be solved by differential quadrature method. Peng and Li (2010) presented a novel method for analyzing steady thermal stresses in a functionally graded hollow cylinder. The thermal and thermoelastic parameters are assumed to arbitrarily vary along the radial direction of the hollow cylinder. The BVP associated with a thermoelastic problem is converted to a Fredholm integral equation. By numerically solving the resulting equation, the distribution of the thermal stresses and radial displacement is obtained. Afshar et al. (2011) studied a glass-like (viscoelastic) functionally graded cylinder by using finite element method to investigate the mechanical responses. A subroutine is developed by using ANSYS parametric design language (APDL) to simulate two nonlinearities, which are the variation of material properties with respect to time and position.

In this paper, governing elasticity equations of a simply (diaphragm) supported symmetric FG orthotropic cylinder are used to predict its behaviour under longitudinally sinusoidal thermal load. Material constants are assumed to have a power-law dependence on the radial coordinate. By assuming a global analytical solution in the longitudinal direction satisfying the two end boundary conditions exactly, the 2D problem is reduced to a 1D problem in the radial direction. The equations are reformulated to enable application of an efficient and accurate numerical integration technique for the solution of the BVP of a cylinder in the radial coordinate. To enable application of numerical integration, BVP of a cylinder is converted into a set of initial value problems (IVPs). The basic approach to convert a BVP into a set of IVPs is also explained in the following sections. Finally, a comparison of the resulting stresses with the elasticity plane strain solution of infinitely long cylinder (Ye et al. 2001) is carried out for ratios of the inner radius to outer radius of 1.5 and 1.05 and for two ratios of length to inner radius, viz., 2 and 100. Results are validated through comparison with those given by Ye et al. (2001).

In addition, one dimensional elasticity equations of an infinitely long axisymmetric cylinder are utilized to reformulate the mathematical model suitable for numerical integration. These equations are summarized in the Appendix. This has been done with a view to check and compares the results of the present formulation of finite length cylinder under uniform internal/external thermal and mechanical loads, when the length of the cylinder tends to infinity.

2 Mathematical model

Basic governing equations of a 2D problem of a cylinder in cylindrical coordinates (Fig. 1a) are:

Equilibrium equations

$$\frac{\partial \sigma_r}{\partial r}+\frac{\partial \tau_{zr}}{\partial z}+\frac{\sigma_r-\sigma_\theta}{r}=0,\quad \frac{\partial \tau_{zr}}{\partial r}+\frac{\partial \sigma_z}{\partial z}+\frac{\tau_{zr}}{r}=0 \tag{2a}$$

Strain displacement relations

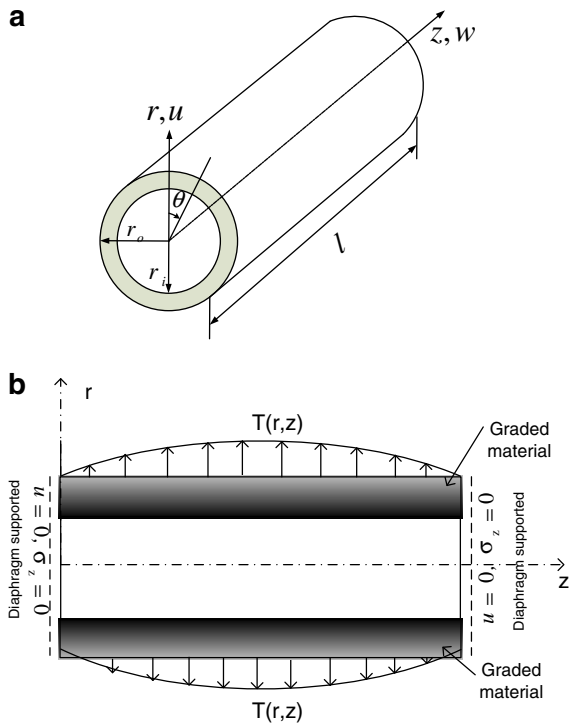

Fig. 1 **a** Coordinate system and geometry of cylinder. **b** Finite FG cylinder under sinusoidal external thermal loading

$$\varepsilon_r = \frac{\partial u}{\partial r} \quad \varepsilon_\theta = \frac{u}{r} \quad \varepsilon_z = \frac{\partial w}{\partial z} \quad \gamma_{zr} = \frac{\partial w}{\partial r} + \frac{\partial u}{\partial z} \tag{2b}$$

Stress–strains–temperature relations for cylindrically orthotropic material

$$\begin{aligned}
\varepsilon_r &= \frac{\sigma_r}{E_r} - \upsilon_{\theta r}\frac{\sigma_\theta}{E_\theta} - \upsilon_{zr}\frac{\sigma_z}{E_z} + \alpha_r T,\\
\varepsilon_\theta &= -\upsilon_{r\theta}\frac{\sigma_r}{E_r} + \frac{\sigma_\theta}{E_\theta} - \upsilon_{z\theta}\frac{\sigma_z}{E_z} + \alpha_\theta T,\\
\varepsilon_z &= -\upsilon_{rz}\frac{\sigma_r}{E_r} - \upsilon_{\theta z}\frac{\sigma_\theta}{E_\theta} + \frac{\sigma_z}{E_z} + \alpha_z T, \quad \gamma_{rz} = \frac{\tau_{rz}}{G_{rz}},
\end{aligned} \tag{2c}$$

Stresses in terms of strains can be written as follows

$$\begin{Bmatrix} \sigma_r \\ \sigma_\theta \\ \sigma_z \\ \tau_{rz} \end{Bmatrix} = \begin{bmatrix} C_{11} & C_{12} & C_{13} & 0 \\ C_{21} & C_{22} & C_{23} & 0 \\ C_{31} & C_{32} & C_{33} & 0 \\ 0 & 0 & 0 & C_{44} \end{bmatrix} \begin{Bmatrix} \varepsilon_r - \alpha_r T \\ \varepsilon_\theta - \alpha_\theta T \\ \varepsilon_z - \alpha_z T \\ \gamma_{rz} \end{Bmatrix} \tag{2d}$$

where, $\upsilon_{r\theta} = \frac{\upsilon_{\theta r}}{E_\theta} E_r, \quad \upsilon_{rz} = \frac{\upsilon_{zr}}{E_z} E_r, \quad \upsilon_{z\theta} = \frac{\upsilon_{\theta z}}{E_\theta} E_z$

$$C_{11} = \frac{E_r(1-\upsilon_{\theta z}\upsilon_{z\theta})}{\Delta}, \quad C_{12} = \frac{E_r(\upsilon_{\theta r}+\upsilon_{zr}\upsilon_{\theta z})}{\Delta},$$
$$C_{13} = \frac{E_r(\upsilon_{zr}+\upsilon_{\theta r}\upsilon_{z\theta})}{\Delta}, C_{22} = \frac{E_\theta(1-\upsilon_{rz}\upsilon_{zr})}{\Delta},$$
$$C_{32} = \frac{E_\theta(\upsilon_{z\theta}+\upsilon_{r\theta}\upsilon_{zr})}{\Delta}, \quad C_{33} = \frac{E_z(1-\upsilon_{r\theta}\upsilon_{\theta r})}{\Delta}$$
$$\text{where } \Delta = (1 - v_{r\theta}v_{\theta r} - v_{\theta z}v_{z\theta} - v_{zr}v_{rz} - 2v_{\theta r}v_{z\theta}v_{rz})$$
$$C_{21} = C_{12},\ C_{23} = C_{32},\ C_{31} = C_{13},\ C_{44} = G \tag{2e}$$

It is assumed that all material constants have a power-law dependence on the radial coordinate, i.e.,

$$C_{ij} = C_{ij}^0 \xi^n, \quad \alpha_i = \alpha_i^0 \xi^n \tag{2f}$$

where $\xi = \frac{r}{r_i}$, C_{ij}^0, and α_i^0 are constants, and n is a inhomogeneity parameter or gradient index. Spatial variation of Poisson's ratio is of much less practical significance than that of Young's modulus. Poisson's ratio is thus assumed to be a constant. This assumption, commonly made in the literature on FGMs, leads to considerable mathematical simplification. It can be easily proved that when the material is isotropic and if $n = 0$ for the homogeneous case, without taking thermal effect, results are same as given by Timoshenko and Goodier (1951) for plane strain elasticity solution for Lame cylinder.

Stresses in terms of displacement components can be cast as follows:

$$\begin{aligned}
\sigma_r &= C_{11}\left(\frac{\partial u}{\partial r} - \alpha_r T\right) + C_{12}\left(\frac{u}{r} - \alpha_\theta T\right) + C_{13}\left(\frac{\partial w}{\partial z} - \alpha_z T\right)\\
\sigma_\theta &= C_{21}\left(\frac{\partial u}{\partial r} - \alpha_r T\right) + C_{22}\left(\frac{u}{r} - \alpha_\theta T\right) + C_{23}\left(\frac{\partial w}{\partial z} - \alpha_z T\right)\\
\sigma_z &= C_{31}\left(\frac{\partial u}{\partial r} - \alpha_r T\right) + C_{32}\left(\frac{u}{r} - \alpha_\theta T\right) + C_{33}\left(\frac{\partial w}{\partial z} - \alpha_z T\right)\\
\tau_{rz} &= C_{44}\gamma_{rz} = C_{44}\left(\frac{\partial w}{\partial r} + \frac{\partial u}{\partial z}\right)
\end{aligned} \tag{2g}$$

and boundary conditions (Fig. 1b) in the longitudinal and radial directions are written in Eq. 3 as,

$$\begin{aligned}
&\text{at } z = 0,\ l; \quad u = \sigma_z = 0; \quad \text{at } r = r_i,\ r_o;\\
&\sigma_r = \tau_{rz} = 0
\end{aligned} \tag{3}$$

in which l is the length, r_i is the inner radius and r_o is the outer radius of a hollow cylinder.

Radial direction r is chosen to be a preferred independent coordinate. Four fundamental dependent variables, viz., displacements, u and w and corresponding stresses, σ_r and τ_{rz} that occur naturally on a

tangent plane $r =$ constant, are chosen in the radial direction. Circumferential stress σ_θ and axial stress σ_z are treated here as auxiliary variables since these are found to be dependent on the chosen fundamental variables (Kant and Ramesh 1981). A set of four first order partial differential equations in independent coordinate r which involves only fundamental variables is obtained through algebraic manipulation of Eqs. 2a–2g. These are,

$$\frac{\partial u}{\partial r} = \frac{\sigma_r}{C_{11}} + \alpha_r T + \frac{C_{12}}{C_{11}}\left(\alpha_\theta T - \frac{u}{r}\right) + \frac{C_{13}}{C_{11}}\left(\alpha_z T - \frac{\partial w}{\partial z}\right),$$
$$\frac{\partial w}{\partial r} = \frac{1}{C_{44}}\tau_{rz} - \frac{\partial u}{\partial z}$$

$$\frac{\partial \sigma_r}{\partial r} = -\frac{\partial \tau_{rz}}{\partial z} + \frac{\sigma_r}{r}\left(\frac{C_{21}}{C_{11}} - 1\right) + \left(\frac{C_{21}C_{12}}{C_{11}} - C_{22}\right) \times \left(\frac{\alpha_\theta T}{r} - \frac{u}{r^2}\right) + \left(\frac{C_{21}C_{13}}{C_{11}} - C_{23}\right)\left(\frac{\alpha_z T}{r} - \frac{1}{r}\frac{\partial w}{\partial z}\right) \tag{4a}$$

$$\frac{\partial \tau_{rz}}{\partial r} = -\frac{\tau_{rz}}{r} - \frac{C_{31}}{C_{11}}\frac{\partial \sigma_r}{\partial z} - C_{31}\frac{\partial(\alpha_r T)}{\partial z} + \left(C_{32} - \frac{C_{12}C_{31}}{C_{11}}\right)\frac{\partial}{\partial z}\left(\alpha_\theta T - \frac{u}{r}\right) + \left(C_{33} - \frac{C_{13}C_{31}}{C_{11}}\right)\frac{\partial}{\partial z}\left(\alpha_z T - \frac{\partial w}{\partial z}\right)$$

and the auxiliary variables,

$$\sigma_\theta = C_{21}\left(\frac{\partial u}{\partial r} - \alpha_r T\right) + C_{22}\left(\frac{u}{r} - \alpha_\theta T\right) + C_{23}\left(\frac{\partial w}{\partial z} - \alpha_z T\right)$$
$$\sigma_z = C_{31}\left(\frac{\partial u}{\partial r} - \alpha_r T\right) + C_{32}\left(\frac{u}{r} - \alpha_\theta T\right) + C_{33}\left(\frac{\partial w}{\partial z} - \alpha_z T\right) \tag{4b}$$

A longitudinally sinusoidal variation of temperature is assumed as follows,

$$T(r,z) = T_{\mathrm{m}} \sin\frac{\pi z}{l} \tag{5a}$$

Variations of the four fundamental dependent variables which completely satisfy the boundary conditions of simple (diaphragm) supports at $z = 0$, l can then be assumed as,

$$\begin{aligned} u(r,z) &= U(r)\sin\tfrac{\pi z}{l} & \sigma_r(r,z) &= \sigma(r)\sin\tfrac{\pi z}{l} \\ w(r,z) &= W(r)\cos\tfrac{\pi z}{l}, & \tau_{rz}(r,z) &= \tau(r)\cos\tfrac{\pi z}{l} \end{aligned} \tag{5b}$$

Substitution of Eqs. 5a and 5b in Eq. 4a, b and simplification resulting from orthogonality conditions of trigonometric functions lead to the following four simultaneous ODEs involving only fundamental variables. These are,

$$U'(r) = \frac{\sigma(r)}{C_{11}} + \alpha_r T_{\mathrm{m}} + \frac{C_{12}}{C_{11}}\left(\alpha_\theta T_{\mathrm{m}} - \frac{U(r)}{r}\right) + \frac{C_{13}}{C_{11}}\left(\alpha_z T_{\mathrm{m}} + \frac{\pi}{l}W(r)\right),$$
$$W'(r) = \frac{1}{G}\tau(r) - U(r)\frac{\pi}{l}$$
$$\sigma'(r) = \frac{\pi}{l}\tau(r) + \left(\frac{C_{21}}{C_{11}} - 1\right)\frac{\sigma(r)}{r} + \left(\frac{C_{21}C_{12}}{C_{11}} - C_{22}\right)\left(\frac{\alpha_\theta}{r}T_{\mathrm{m}} - \frac{U(r)}{r^2}\right) + \left(\frac{C_{21}C_{13}}{C_{11}} - C_{23}\right)\left(\frac{\alpha_z}{r}T_{\mathrm{m}} + \frac{\pi}{l}\frac{W(r)}{r}\right)$$
$$\tau'(r) = -\frac{\tau(r)}{r} - \frac{\pi}{l}\frac{C_{31}}{C_{11}}\sigma(r) - C_{31}\left(\alpha_r\frac{\pi}{l}T_{\mathrm{m}}\right) + \left(C_{32} - \frac{C_{12}C_{31}}{C_{11}}\right)\left(\alpha_\theta\frac{\pi}{l}T_{\mathrm{m}} - \frac{\pi}{l}\frac{U(r)}{r}\right) + \left(C_{33} - \frac{C_{13}C_{31}}{C_{11}}\right)\left(\alpha_z\frac{\pi}{l}T_{\mathrm{m}} + \left(\frac{\pi}{l}\right)^2 W(r)\right) \tag{6a}$$

and the auxiliary variables,

$$\sigma_\theta = \left[\frac{C_{21}}{C_{11}}\sigma(r) + \left(\frac{C_{21}C_{12}}{C_{11}} - C_{22}\right)\left(\alpha_\theta T_{\mathrm{m}} - \frac{U(r)}{r}\right) + \left(\frac{C_{13}C_{21}}{C_{11}} - C_{23}\right)\left(\alpha_z T_{\mathrm{m}} + \frac{\pi}{l}W(r)\right)\right]\sin\frac{\pi z}{l}$$
$$\sigma_z = \left[\frac{C_{31}}{C_{11}}\sigma(r) + \left(\frac{C_{31}C_{12}}{C_{11}} - C_{32}\right)\left(\alpha_\theta T_{\mathrm{m}} - \frac{U(r)}{r}\right) + \left(\frac{C_{13}C_{31}}{C_{11}} - C_{33}\right)\left(\alpha_z T_{\mathrm{m}} + \frac{\pi}{l}W(r)\right)\right]\sin\frac{\pi z}{l} \tag{6b}$$

3 Numerical solution

The above system of first order simultaneous ODEs (6a) together with the appropriate boundary conditions (3) at the inner and outer edges of the cylinder forms a two-point BVP. However, a BVP in ODEs cannot be numerically integrated as only a half of the dependent variables (two) are known at the initial edge and numerical integration of an ODE is intrinsically an IVP. It becomes necessary to transform the problem into a set of IVPs. The

initial values of the remaining two fundamental variables must be selected so that the complete solution satisfies the two specified conditions at the terminal boundary (Kant and Ramesh 1981). The Nth ($N = 4$ here) order BVP is transformed into a set of ($N/2 + 1$) IVPs. ODEs are integrated from initial edge to final edge using the initial values specified in Table 1. The $N/2 + 1$ solutions given in the Table 1 may be thought of as (i) one non-homogeneous integration which includes all the non-homogeneous terms (e.g., loading) and the known $N/2$ quantities at starting edge, with the unknown $N/2$ quantities at the starting edge set equal to zero, (ii) $N/2$ homogeneous integrations which are carried out by setting the known quantities at the starting edge as zero and choosing the $N/2$ unknown quantities at starting edge as unit values in succession and deleting the non-homogeneous terms from the ODEs. The solutions at the terminal boundary corresponding to the initial values are given in the right side columns in Table 1. A linear combination of the ($N/2 + 1$) solutions must satisfy the boundary conditions at the terminal edge, i.e.,

$$\begin{Bmatrix} Y_{3,0} \\ Y_{4,0} \end{Bmatrix} + \begin{pmatrix} Y_{3,1} & Y_{3,2} \\ Y_{4,1} & Y_{4,2} \end{pmatrix} \begin{pmatrix} X_1 \\ X_2 \end{pmatrix} = \begin{Bmatrix} \overline{Y_3} \\ \overline{Y_4} \end{Bmatrix}$$
$$Y_{i,0} + Y_{i,j}X_j = \overline{Y_i} \qquad (7)$$
$$\text{or} \qquad \text{or}$$
$$X_j = \left[Y_{i,j}\right]^{-1}\left(\overline{Y_i} - Y_{i,0}\right)$$

where i indicates the $N/2$ variables consistent with the specified boundary values at terminal edge, j refers to solution number and ranges from 1 to $N/2$, $\overline{Y_i}$ is a vector of specified dependent variables at the terminal boundary and X_j is a vector of unknown dependent variables at the starting edge. Finally, a non-homogeneous integration with all the dependent variables known at the starting edge is carried out to get the desired results. Fourth order Runge–Kutta algorithm with modifications suggested by Gill (1951) is used for the numerical integration of the IVPs. Flow chart for numerical integration is shown in the Fig. 2.

Table 1 Initial and integrated values

IN	Initial boundary				Terminal boundary				Load term
	u	w	σ_r	τ_{rz}	u	w	σ_r	τ_{rz}	
0	0	0	0 (S)	0 (S)	$Y_{1,0}$	$Y_{2,0}$	$Y_{3,0}$	$Y_{4,0}$	I
1	1	0	0	0	$Y_{1,1}$	$Y_{2,1}$	$Y_{3,1}$	$Y_{4,1}$	D
2	0	1	0	0	$Y_{1,2}$	$Y_{2,2}$	$Y_{3,2}$	$Y_{4,2}$	D
FI	X_1	X_2	0 (S)	0 (S)	C	C	C	C	I

IN integration number, *S* specified, *C* correct value, *FI* final integration, *I* include, *D* delete

4 Results and discussion

Nondimensionalized parameters are defined as follows in Eq. 8:

$$\overline{r} = \frac{r}{R}, \quad R = \frac{1}{2}(r_o + r_i), \quad (\overline{u}, \overline{w}) = \frac{1}{\alpha t_r^o TR}(u, w),$$
$$\left(\overline{\sigma_r}, \overline{\sigma_\theta}, \overline{\sigma_z}, \overline{\tau_{rz}}\right) = \frac{1}{\alpha t_r^o TC_{11}^o}\left(\sigma_r, \sigma_\theta, \sigma_z, \tau_{rz}\right) \qquad (8)$$

A hollow cylinder is analysed by taking two r_o/r_i ratios, 1.05 and 1.5, which cover both thick and thin cases. Material properties for transversely isotropic material are taken as follows (Ye et al. 2001).

Material I

$$C_{12}^o/C_{11}^o = 0.364, \quad C_{13}^o/C_{11}^o = 0.372,$$
$$C_{33}^o/C_{11}^o = 1.002, \quad \alpha_3^o/\alpha_1^o = 1.010$$

Material II

$$C_{12}^o/C_{11}^o = 0.5, \quad C_{13}^o/C_{11}^o = 0.2,$$
$$C_{33}^o/C_{11}^o = 3.2, \quad \alpha_3^o/\alpha_1^o = 2.6$$

Using above relations between the material constants following properties are taken for numerical analysis.

Material I

$$C_{11}^o = 22.29 \times 10^6, \quad C_{12}^o = 8.1135 \times 10^6,$$
$$C_{13}^o = 8.2918 \times 10^6,$$
$$C_{21}^o = 8.1135 \times 10^6, \quad C_{22}^o = 22.29 \times 10^6,$$
$$C_{23}^o = 8.2918 \times 10^6,$$
$$C_{31}^o = 8.2918 \times 10^6, \quad C_{32}^o = 8.2918 \times 10^6,$$
$$C_{33}^o = 22.33 \times 10^6,$$
$$C_{44}^o = 8.272 \times 10^6$$
$$\alpha_r = 51 \times 10^{-6}, \quad \alpha_\theta = 51 \times 10^{-6},$$
$$\alpha_z = 5.151 \times 10^{-5}$$

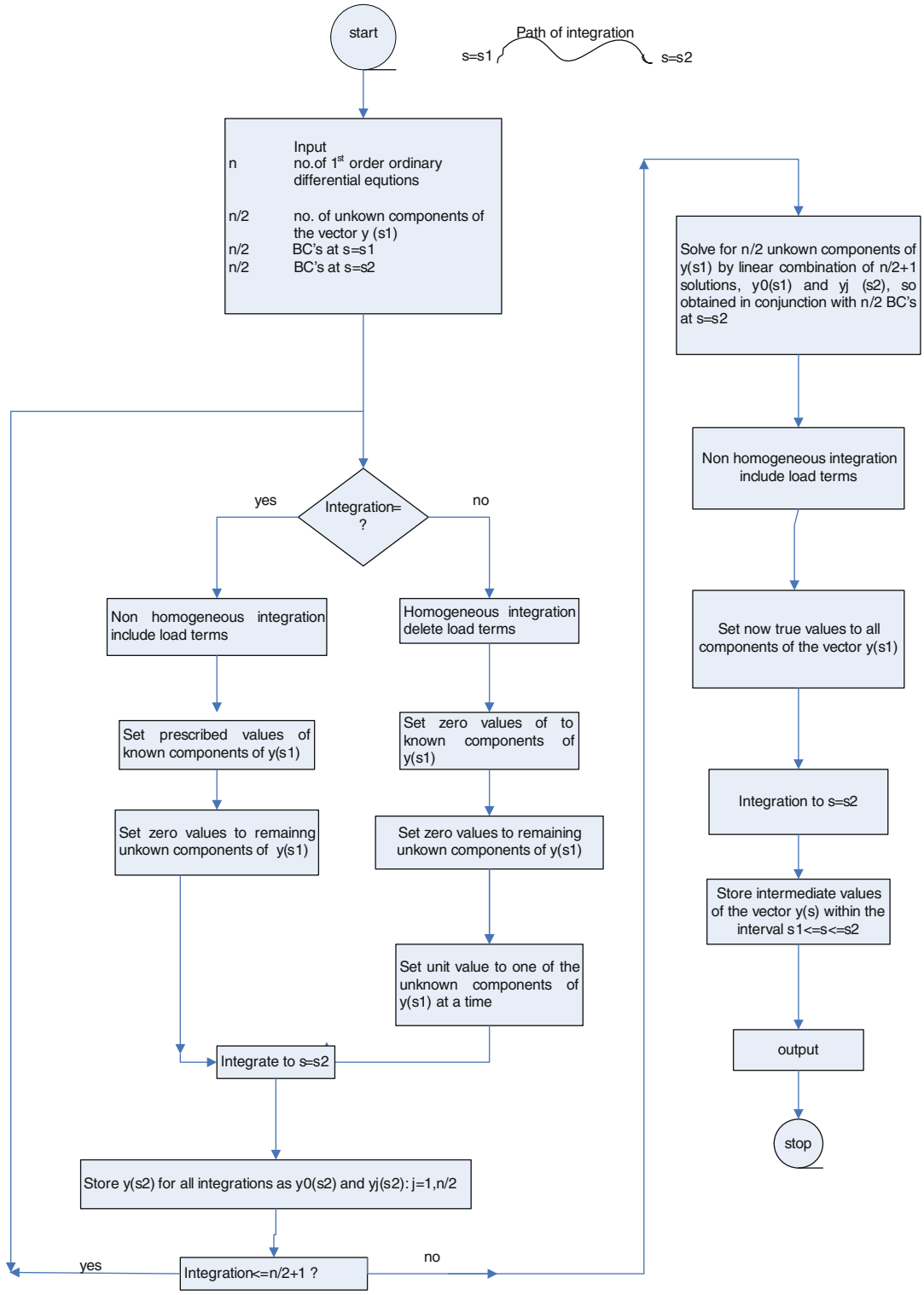

Fig. 2 Flowchart for numerical integration

Material II

$C^{o}_{11} = 22.29 \times 10^{6}$, $C^{o}_{12} = 11.14 \times 10^{6}$, $C^{o}_{13} = 4.46 \times 10^{6}$,

$C^{o}_{21} = 11.14 \times 10^{6}$, $C^{o}_{22} = 22.29 \times 10^{6}$, $C^{o}_{23} = 4.46 \times 10^{6}$,

$C^{o}_{31} = 4.46 \times 10^{6}$, $C^{o}_{32} = 4.46 \times 10^{6}$, $C^{o}_{33} = 71.32 \times 10^{6}$,

$C^{o}_{44} = 8.272 \times 10^{6}$

$\alpha_r = 51 \times 10^{-6}$, $\alpha_\theta = 51 \times 10^{-6}$, $\alpha_z = 1.33 \times 10^{-4}$

Numerical analysis is carried out with both material I and material II, various inhomogeneity parameters $n = 2$, 1 and -2 and two l/r_i ratios 2 and 100. Figures 3, 4, 5, 6, 7, and 8 show the variations of basic fundamental variables as well as auxiliary variables through thickness for r_o/r_i ratio of 1.5 signifying a thick cylinder and Figs. 9 and 10 show the variation of basic fundamental variable radial stress as well as auxiliary variable hoop stress through thickness for r_o/r_i ratio 1.05. Radial and hoop quantities are maximum at $z = l/2$ whereas axial quantities are maximum at $z = 0, l$.

Table 2 shows values of radial, hoop and axial stresses for $l/r_i = 2$ and 100. These values are compared with those of Ye et al. (2001) for plane strain elasticity solution for infinitely long cylinder in Table 2. For $l/r_i = 100$, results are close to those of Ye et al. (2001). Axial displacement is constant over the thickness for both r_o/r_i ratios. Radial displacement is linear through thickness; gives higher value for

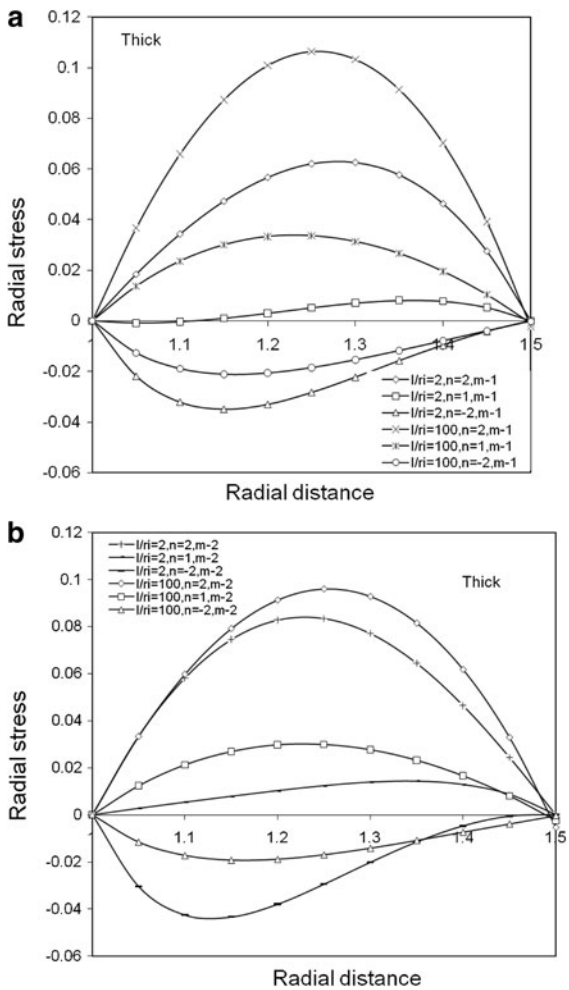

Fig. 3 Distribution of $\overline{\sigma}_r$ through thickness for $r_o/r_i = 1.5$ for **a** material I and **b** material II

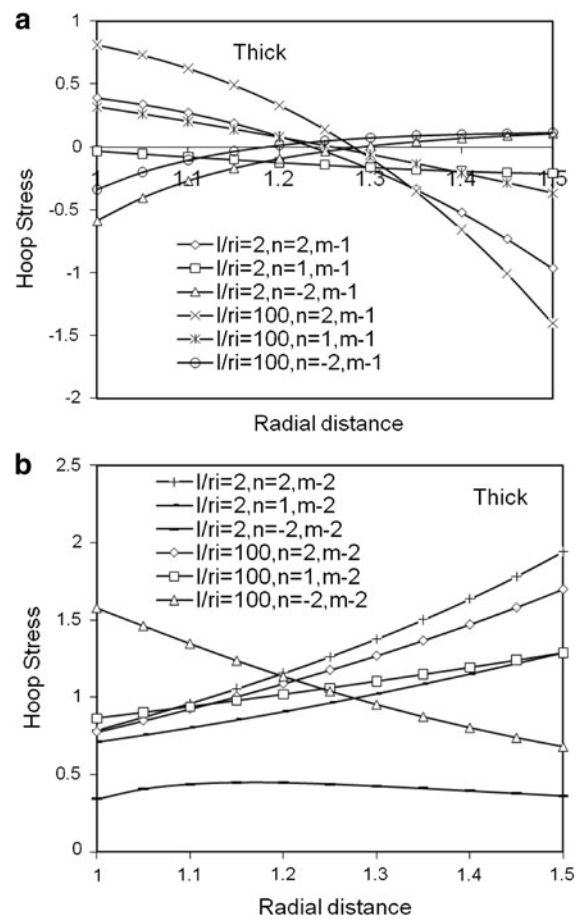

Fig. 4 Distribution of $\overline{\sigma}_\theta$ through thickness for $r_o/r_i = 1.5$ for **a** material I and **b** material II

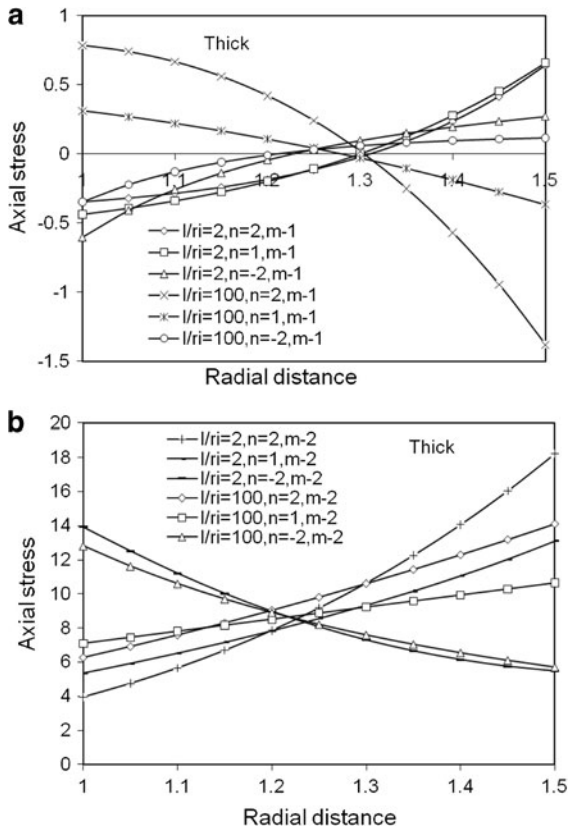

Fig. 5 Distribution of $\overline{\sigma}_z$ through thickness for $r_o/r_i = 1.5$ for **a** material I and **b** material II

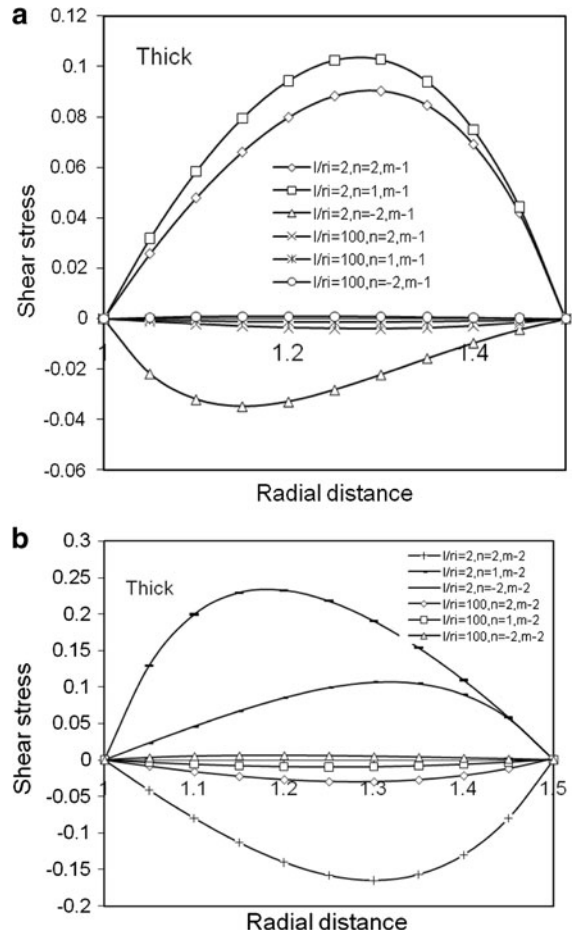

Fig. 6 Distribution of $\overline{\tau}_{rz}$ through thickness for $r_o/r_i = 1.5$ for **a** material I and **b** material II

positive n as compared to negative n. Parabolic variations of shear stress and radial stress are seen in both thin and thick cases. In thin cylinder, hoop and axial stresses have linear variation and nonlinear parabolic through thickness in thick cylinder. From Fig. 3a, it is seen that positive value of n produces positive magnitude of radial stress ($n = 2, 1$) whereas negative value of $n = -2$ gives negative radial stress for both $l/r_i = 2, 100$. Both l/r_i ratio follow similar trend, whereas opposite behavior is seen for non homogeneity parameter $n = 2$ and $n = -2$. Figure 3b shows radial stress results for material property II. There is no significant effect is seen in terms of trends of radial stress through thickness for both material properties. Figure 4a gives nonlinear behavior of hoop stress for $n = 2, 1$, it gives variation from positive to negative (higher to lower) whereas $n = -1$ gives variation lower to higher values. From Fig. 4b it is seen that all positive hoop stress is obtained for all cases for material II. Negative values of nonhomogeneity give drastic behavior change in the magnitude. From, Fig. 5a, it is seen that there is a effect of l/r_i ratios on axial stresses unlike for radial stresses. Similarly from, Fig. 6a, b, it is seen the effect of l/r_i ratios on stresses. Parabolic shear stresses are obtained for both cases. From Fig. 7a, it is seen that radial displacement is linear. Effect of n is seen for $n = 2$, $n = -1$ and $n = -2$. $n = 2$ gives higher range of stresses, it decreases with $n = 1$ and gradually further decreases for $n = -2$. Similar is the case for material II (Fig. 7b). Constant values are obtained for axial displacements as seen from Fig. 8a. Negligible and lower values are obtained for $l/r_i = 2$ whereas higher values are obtained for $l/r_i = 100$. Same is the case for material properties II (Fig. 8b). From Fig. 9a, b shows radial stresses for thin cylinder. For different n values, behavior of thin cylinder is same as thick

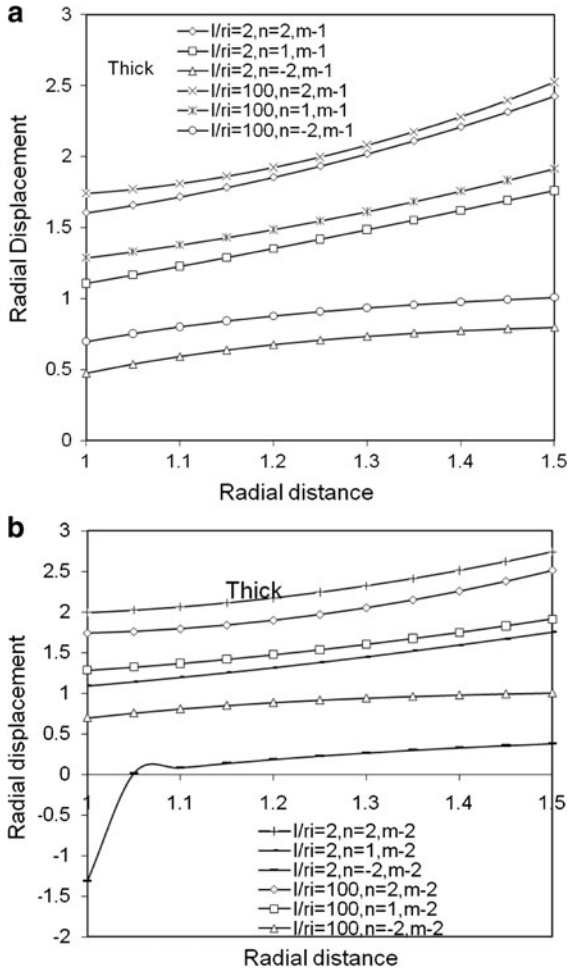

Fig. 7 Distribution of $\overline{u}$ through thickness for $r_o/r_i = 1.5$ for **a** material I and **b** material II

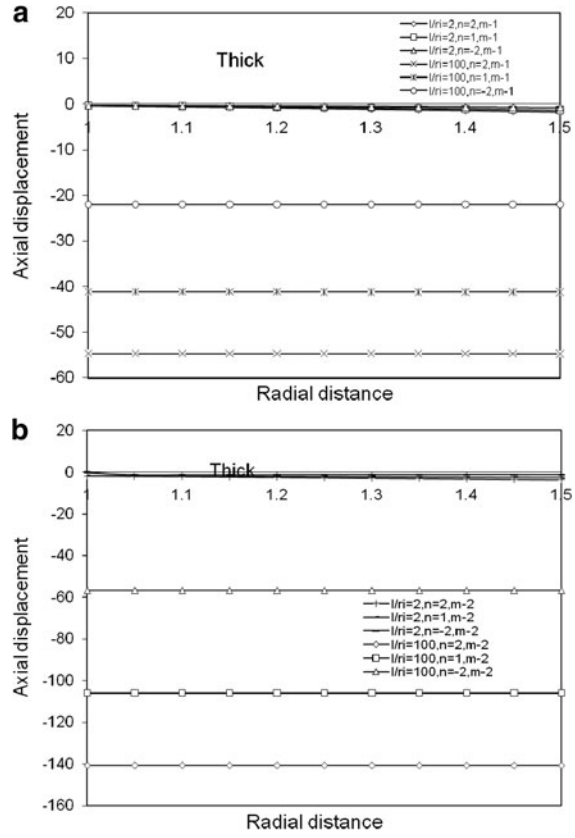

Fig. 8 Distribution of $\overline{w}$ through thickness for $r_o/r_i = 1.5$ for **a** material I and **b** material II

cylinder. From Fig. 10a, b, it is seen that hoop stresses are linearly varying as compared to ratio thick cylinder. It is seen that non-homogeneity parameter n both positive and negative has greater effect on distribution of stresses and displacements. Stresses can be triggered easily with functionally graded model presented according to the engineering design requirements.

5 Conclusion

An attempt is made here to analyze the FG cylinders which are subjected to elastostatic and temperature fields through exact semi analytical cum numerical approach which differs from conventional approximate finite element approach and is also free from any assumptions in the theory. Results are very useful when one is designing pressurized cylinders made up of FG materials subjected to thermal load. This approach can be applied to very thick cylinders. Technique is very convenient to obtain the stresses with an ease, since no separate integration is required to account the non homogeneity effect occurred due to gradation. This is an important feature of the proposed model. Also, it involves mixed variables in the derivations, both stresses and displacements are obtained accurately simultaneously. Systematic development of mathematical model has significantly contributed in understanding the behavioural phenomenon of graded cylinders under extreme loading environment of thermal loadings. Mathematical model developed here is simple in nature and easily applicable for the large class of shell problems. Choice of fundamental variables is an important task for developing the model. Current model is applicable to simply diaphragm supported cylinder only. Change in

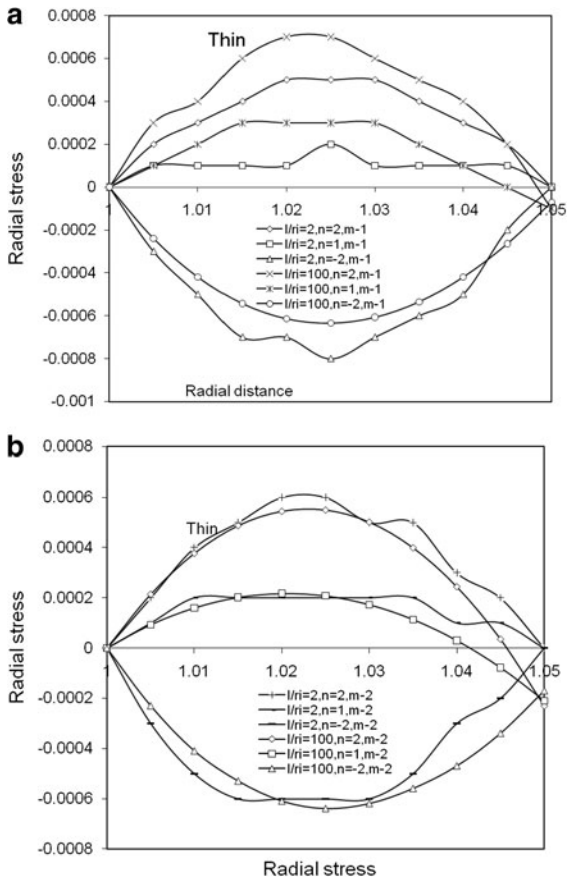

Fig. 9 Distribution of $\overline{\sigma}_r$ through thickness for $r_o/r_i = 1.05$ for **a** material I and **b** material II

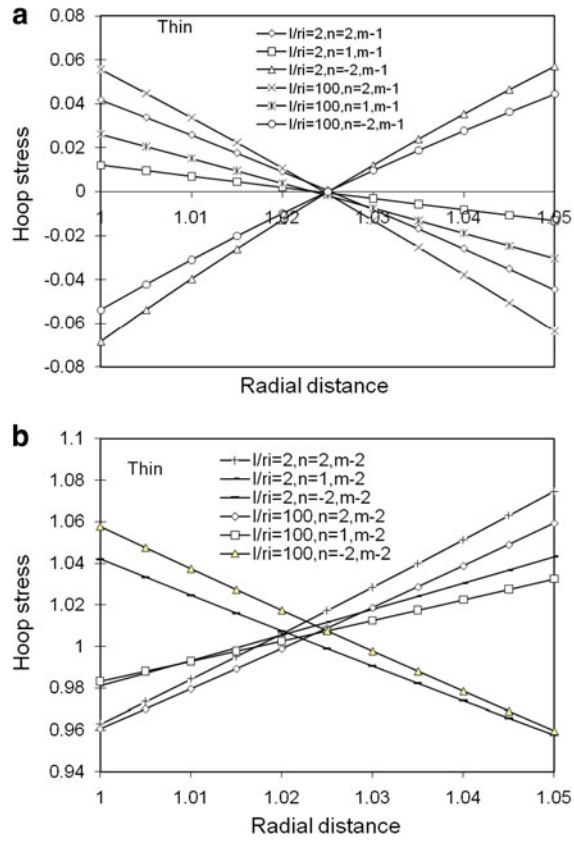

Fig. 10 Distribution of $\overline{\sigma}_\theta$ through thickness for $r_o/r_i = 1.05$ for **a** material I and **b** material II

Table 2 Comparison of non-dimensional radial stress $\overline{\sigma_r}\,(z = l/2)$, hoop stress $\overline{\sigma_\theta}\,(z = l/2)$ and axial stress $\overline{\sigma_z}\,(z = 0,\ l)$ through thickness for $l/r_i = 1.5$, material I and $n = 2$ for diaphragm supported elastic orthotropic cylinder under thermal load with elasticity plane strain solutions given by Ye et al. (2001)

Quantity	r/r_i	Present numerical solutions—finite length cylinder		Analytical elasticity plane strain solution by Ye et al. (2001) and numerical solution for plane strain infinitely long cylinder
		$l/r_i = 2$	$l/r_i = 100$	
$\overline{\sigma_r}\,(z = l/2)$	1.05	0.0184	0.0367	0.0376
	1.2	0.0567	0.1009	0.101225
	1.25	0.0621	0.1064	0.108365
	1.3	0.0626	0.1033	0.105184
	1.4	0.0463	0.0702	0.070456
$\overline{\sigma_\theta}\,(z = l/2)$	1.0	0.3896	0.8099	0.823538
	1.05	0.338	0.7286	0.746013
	1.1	0.2711	0.6233	0.641465
	1.4	−0.5234	−0.6588	−0.65224
	1.5	−0.9663	−1.4031	−1.35085
$\overline{\sigma_z}\,(z = 0,\ l)$	1.2	−0.1862	0.4201	0.392654
	1.15	−0.2423	0.5609	0.476166
	1.25	−0.1148	0.2405	0.307495

Fourier series expansion can be extended to tackle other boundary conditions that can be considered as limitation of the current model. Numerical results presented for different r_o/r_i and l/r_i ratios will be useful for future reference and can be used as benchmark results.

Appendix: 1D formulation for orthotropic cylinder under thermal loading

$$\frac{d\sigma_r}{dr}+\frac{1}{r}(\sigma_r-\sigma_\theta)=0,\quad \varepsilon_r=\frac{\partial u}{\partial r},\quad \varepsilon_\theta=\frac{u}{r},\tag{9}$$

$$\begin{aligned}\sigma_r &= C_{11}(\varepsilon_r-\alpha_r T)+C_{12}(\varepsilon_\theta-\alpha_\theta T)\\ \sigma_\theta &= C_{12}(\varepsilon_r-\alpha_r T)+C_{22}(\varepsilon_\theta-\alpha_\theta T)\end{aligned},$$

$$\begin{aligned}\sigma_r &= C_{11}\tfrac{du}{dr}-C_{11}\alpha_r T+C_{12}\tfrac{u}{r}-C_{12}\alpha_\theta T\\ \sigma_\theta &= C_{21}\tfrac{du}{dr}-C_{21}\alpha_r T+C_{22}\tfrac{u}{r}-C_{22}\alpha_\theta T\end{aligned},$$

$$\begin{aligned}\frac{du}{dr} &= \frac{\sigma_r}{C_{11}}+\alpha_r T-\frac{C_{12}}{C_{11}}\frac{u}{r}+\frac{C_{12}}{C_{11}}\alpha_\theta T,\\ \frac{d\sigma_r}{dr} &= \frac{\sigma_r}{r}\left(\frac{C_{21}}{C_{11}}-1\right)+\frac{u}{r^2}\left(C_{22}-\frac{C_{21}C_{12}}{C_{11}}\right)\\ &\quad+\frac{\alpha_\theta T}{r}\left(\frac{C_{21}C_{12}}{C_{11}}-C_{22}\right)\end{aligned}\tag{10}$$

where,

$$\upsilon_{r\theta}=\frac{\upsilon_{\theta r}}{E_\theta}E_r,\quad C_{11}=\frac{E_r}{(1-\upsilon_{r\theta}\upsilon_{\theta r})},$$
$$C_{12}=\frac{\upsilon_{r\theta}E_\theta}{(1-\upsilon_{r\theta}\upsilon_{\theta r})},\quad C_{22}=\frac{E_\theta}{(1-\upsilon_{r\theta}\upsilon_{\theta r})},$$
$$C_{21}=C_{12},\quad C_{ij}=C_{ij}^0\xi^n,\quad \alpha_i=\alpha_i^0\xi^n$$

References

Afshar, R., Bayat, M., Lalwani, R.K., Yau, Y.H.: Elastic behavior of glass-like functionally graded infinite hollow cylinder under hydrostatic loads using finite element method. Mater. Des. **32**, 781–787 (2011)

Chen, Y.Z., Lin, X.Y.: An alternative numerical solution of thick-walled cylinders and spheres made of functionally graded materials. Comput. Mater. Sci. **48**, 640–647 (2010)

Chen, W.Q., Ye, G.R., Cai, J.B.: Thermoelastic stresses in a uniformly heated functionally graded isotropic hollow cylinder. J. Zhejiang Univ. Sci. **3**(1), 1–5 (2002)

Desai, P., Kant, T.: Ton accurate stress determination in laminated finite length cylinders subjected to thermoelastic load. Int. J. Mech. Solids **6**(1), 7–26 (2011)

Gill, S.: A process for the step-by-step integration of differential equations in an automatic digital computing machine. Proc. Camb. Philos. Soc. **47**(Part 1), 96–108 (1951)

Goldberg, J.E. Setlur, A.V., Alspaugh, D.W.: Computer analysis of non-circular cylindrical shells. In: Proceedings of the IASS Symposium on Shell Structures in Engineering Practice, Budapest, Hungary (1965)

Horgan, C.O., Chan, A.M.: The pressurized hollow cylinder or disk problem for functionally graded isotropic linearly elastic materials. J. Elast. **55**, 43–59 (1999)

Jabbari, M., Sohrabpour, S., Eslami, M.R.: Mechanical and thermal stresses in a functionally graded hollow cylinder due to radially symmetric loads. Int. J. Press. Vessels Pip. **79**, 493–497 (2002)

Kant, T., Ramesh, C.K.: Numerical integration of linear boundary value problems in solid mechanics by segmentation method. Int. J. Numer. Methods Eng. **17**, 1233–1256 (1981)

Koizumi, M.: FGM activities in Japan. Compos. Part B **28B**, 1–4 (1997)

Kraus, H.: Thin Elastic Shells. Wiley, New York (1967)

Liew, K.M., Kitipornchai, S., Zhang, X.Z., Lim, C.W.: Analysis of the thermal stress behaviour of functionally graded hollow circular cylinders. Int. J. Solids Struct. **40**, 2355–2380 (2003)

Peng, X.L., Li, X.F.: Thermoelastic analysis of a cylindrical vessel of functionally graded materials. Int. J. Press. Vessels Pip. **87**, 203–210 (2010)

Shariyat, M., Nikkhah, M., Kazemi, R.: Exact and numerical elastodynamic solutions for thick-walled functionally graded cylinders subjected to pressure shocks. Int. J. Press. Vessels Pip. **88**, 75–87 (2011)

Timoshenko, S., Goodier, J.N.: Theory of Elasticity. McGraw-Hill, New York (1951)

Tutuncu, K., Ozturk, M.: Exact solutions for stresses in functionally graded pressure vessels. Compos. Part B **32**, 683–686 (2001)

Yas, M.H., Sobhani Aragh, B.: Three-dimensional analysis for thermoelastic response of functionally graded fiber reinforced cylindrical panel. Compos. Struct. **92**, 2391–2399 (2010)

Ye, G.R., Chen, W.Q., Cai, J.B.: A uniformly heated functionally graded cylindrical shell with transverse isotropy. Mech. Res. Commun. **28**(5), 535–542 (2001)

Wu, C.-P., Tsai, T.-C.: Exact solutions of functionally graded piezoelectric material sandwich cylinders by a modified Pagano method. Appl. Math. Model. (2011). doi:10.1016/j.apm.2011.07.077